Molecular Mechanism of Radiationless Deactivation of Aminoanthraquinones through Intermolecular Hydrogen-Bonding Interaction with Alcohols and Hydroperoxides

Tomoyuki Yatsuhashi and Haruo Inoue*

Department of Industrial Chemistry, Faculty of Engineering, Tokyo Metropolitan University, 1-1 Minami-ohsawa, Hachioji, Tokyo 192-03, Japan

Received: February 17, 1997; In Final Form: August 18, 1997[⊗]

The molecular mechanism of radiationless deactivation from the excited singlet state of aminoanthraquinones (AAQ) induced by alcohols and hydroperoxides was investigated by time-resolved picosecond fluorescence measurements. AAQ suffered substantial fluorescence quenching with red shifts of their λ_{max} in benzene solution upon addition of alcohol and hydroperoxide. Primary alcohols exhibited the largest quenching effects among 26 alcohols examined, while tertiary alcohols were least effective. The Stern−Volmer constants were well correlated with the ^{13}C NMR chemical shift of the carbinol carbon atom and the contact molecular surface area of the hydroxyl hydrogen of the quenchers, while it apparently did not depend upon pK_a values. Contact molecular surface area was revealed to be a good quantitative parameter for the steric effect in the intermolecular hydrogen-bonding interaction. The steric factor was dominant in the fluorescence-quenching process, but the electronic factor becomes evident among the molecules having the same steric factor such as benzyl alcohol derivatives, where the Hammet plot showed a good linearity. Fluorescence decay kinetics clearly showed that two emitting levels were involved such as the fluorescent state in benzene and a fully relaxed state in which reorganization of the surrounding alcohol was established. Estimated lifetimes of the fully relaxed states were longer than those in neat alcohol by a factor of 30. The results were interpreted that there were at least two relaxation pathways by alcohol reorganization through the intermolecular hydrogen bond. A specific reorganization of alcohol to AAQ induced relaxation from the fluorescent state in benzene to a relaxed, emissive state and to another relaxed, nonfluorescent state. The latter leads to an efficient radiationless deactivation. The relaxed emissive state corresponds to the excited state of intermolecular hydrogen-bonded species of AAQ with the alcohol in the ground state in which the hydroxyl group of alcohol interacts through an in-plane mode against the carbonyl oxygen of AAQ. Another relaxed nonfluorescent state is formed through an out-of-plane mode interaction between AAQ and the hydroxyl group of alcohol.

Introduction

In the electronic excited state, many molecules have dipole moments larger than in the ground state.[1] The dynamic changes of the dipole sometimes induce formation of a strong hydrogen bond in the excited state.[2] The formation of a tight hydrogen-bonded complex leads to very important phenomena. Two π-conjugated systems show efficient deactivation by forming hydrogen-bonded complexes as observed among aminopyrene[3] or pyrenol[4] and pyridine. The shifting of pyrene's active proton toward pyridine by an intermolecular hydrogen bonding leads to lower ionization potential of pyrenes over 1 eV. Then ultrafast electron transfer occurs in nonpolar solvent even when the electron-transfer reactions are very endergonic as predicted by the usual Marcus theory. The hydrogen-bonding interaction between two π-conjugated systems also plays important roles in triplet−triplet energy transfer as reported for the carbazole and quinoline system[5] and in porphyrins systems.[6] Another crucial case is a system between conjugated and nonconjugated molecules. Aminoanthraquinones (AAQ) are characteristic molecules that exhibit strong intermolecular hydrogen-bonding interaction in the excited state, since the excited states have a strong intramolecular charge-transfer nature.[2] The large electron density on the carbonyl oxygen of AAQ in the excited state strongly promotes an intermolecular hydrogen-bonding interaction with a nonconjugated molecule such as an alcohol. We have reported an efficient deactivation of the excited singlet state of AAQ in ethanol.[2] An intermolecular hydrogen bonding with the hydroxyl group of alcohol was revealed to be a dominant mode of radiationless deactivation to the ground state, and the electronic excited energy was supposed to dissipate through the hydrogen bond as vibrational energy. The findings were supported by many researchers for other AAQ derivatives.[7−11] Moog et al. also reported similar results on aminofluorenone derivatives.[12]

Recently, we have found that not only alcohol but also hydroperoxide quenched the fluorescence of AAQ.[13] With the fluorescence quenching the decomposition of hydroperoxide was observed. The decomposition of hydroperoxide could mean that dissipated energy through the intermolecular hydrogen bond was converted selectively to induce chemical reaction such as bond cleavage. Stern−Volmer analyses for the obtained products show that the decomposition was closely related to the fluorescence-quenching process. From the viewpoints of energy dissipation, upon radiationless deactivation from the electronically excited state the excited energy has generally been accepted to dissipate randomly through the surrounding solvent molecules.[14] The sensitized decomposition of hydroperoxide coupled with radiationless deactivation strongly suggests that the excited energy is not randomly but at least partly selectively transferred to a specific molecule surrounding the chromophore in the case. An investigation of the microscopic molecular mechanism of radiationless deactivation by intermolecular hydrogen-bonding interactions would clarify the problem of whether the energy dissipation is inherently isotropic or aniso-

* To whom correspondence should be addressed. E-mail: inoue-haruo@c.metro-u.ac.jp.

[⊗] Abstract published in *Advance ACS Abstracts,* October 1, 1997.

S1089-5639(97)00581-1 CCC: $14.00

tropic. In this paper, we tried to understand the microscopic molecular mechanism of radiationless deactivation induced by intermolecular hydrogen-bonding interactions on the basis of our previous findings.[2]

Experimental Section

Materials. 2-Piperidino-9,10-anthraquinone (2PAQ) and 2-amino-9,10-anthraquinone (2AAQ) were purified as reported elsewhere.[2] Purity was confirmed by HPLC (ODS, acetonitrile, 220 nm detection). Solid alcohols (diphenylmethanol, 1,2-cyclohexanediol, diphenylethanol, triphenylmethanol) were purified by repeated recrystallization from benzene/hexane mixtures, and liquid alcohols were refluxed over the corresponding magnesium alkoxide or calcium hydride, then fractionally distillated under nitrogen atmosphere. Methanol-d_4 (Isotec, 99.96% D), methanol-d_3 (Nakarai, 99.96% D), and ethanol-*O*-*d* (Aldrich, 99.5%+ D) were used as received. Triphenylmethanol-*O*-*d* was prepared by stirring the benzene solution with deuterium oxide (Merck 99.95%D), then dried in vacuum. *tert*-Butyl hydroperoxide was purified by fractional distillation under reduced pressure for three times. Cumene hydroperoxide was purified by the usual alkali salt method.[15] Benzene was washed with concentrated sulfuric acid, then with water, dilute sodium carbonate aqueous solution, and water followed by drying with calcium chloride, refluxing over benzophenone ketyl, and fractionally distilling under nitrogen atmosphere.

Measurements. Absorption spectra were measured with Shimadzu UV-2100PC spectrophotometer. Steady-state fluorescence spectra were measured by a Hitachi F-4010 spectrofluorometer equipped with Hamamatsu R928 photomultiplier tube. Fluorescence decay and time-resolved fluorescence spectra were measured by a picosecond fluorescence lifetime measurement system (Hamamatsu C4334 streak scope, connected with CHROMEX 250IS polychromater) with a Hamamatsu PLP-02 semiconductor laser (420 nm, fwhm 20 ps, 1.19 mW, 1 MHz) under photon-counting conditions. Fluorescence time profiles were fitted by a convolution method. All measurements were carried out at room temperature.

Contact Molecular Surface Area Calculation. Contact molecular surface area is defined as the van der Waals molecular surface area that is exposed outside and is accessible by another specific probe atom or molecule.[16] A specific probe atom that has a van der Waals radius is rolled on the surface of the corresponding molecule in an optimized geometry, and the unexposed area, which is not accessible, is named the reentrant surface. The oxygen atom of the carbonyl in AAQ was chosen as the specific probe atom in this case, and Gavezzotti−PcMol van der Waals radii (H, 1.15 Å; C, 1.75 Å; N, 1.55 Å; O, 1.40 Å; F, 1.30 Å) were used.[17] The quencher structures were first estimated by molecular mechanics (MM2 parameter was used) and further optimized by MOPAC (Version 94.10, PM3) of the CAChe system on the Macintosh. The calculation of the contact molecular surface area of the hydroxyl hydrogen of quenchers (MS(O*H*)) was done by ARVOMOL, Version 2,[18] on an IBM RS/6000-590, and an MS-DOT algorism[19] was used.

Results and Discussions

Absorption Spectra. Absorption spectra were little influenced by the addition of alcohol under the experimental conditions. On addition of excess alcohol, absorption spectra showed red shifts with isosbestic points (Figure 1). Assuming the change of each spectrum to be the formation of the 1:1 complex between AAQ and ethanol, association constants were

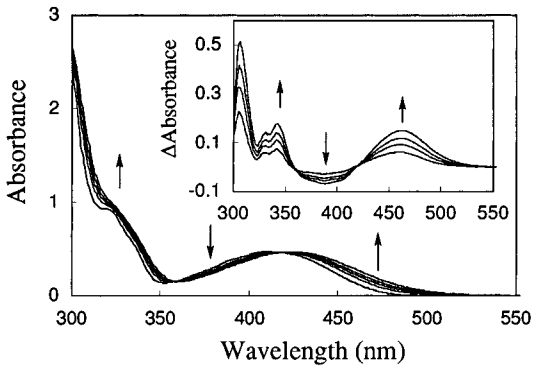

Figure 1. UV−vis absorption spectral changes of 2AAQ upon addition of ethanol. [ethanol] = 0, 0.3, 0.5, 0.7, 1.0 M, and the inset shows those differential spectra.

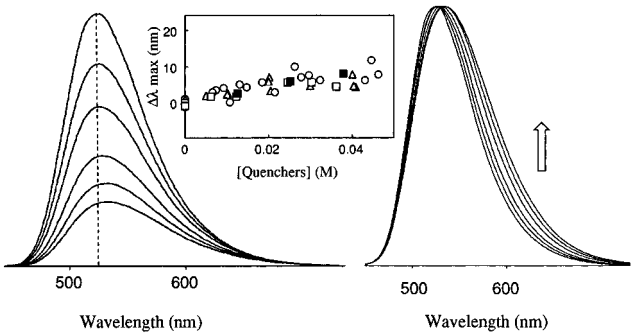

Figure 2. Fluorescence spectra (left) and their normalized spectra (right) of 2AAQ upon addition of ethanol, where [ethanol] = 0−0.05 M and the inset shows the 2AAQ fluorescence λ_{max} dependence on quencher's concentration: (○) primary alcohols; (△) secondary alcohols; (□) tertiary alcohols; (■) hydroperoxides.

calculated to be smaller than 1.0 for 2AAQ and 1.0 for 2PAQ in benzene. Under the experimental conditions of [ethanol] = 0−0.05 M, more than 95% of AAQ exists alone without forming a 1:1 complex with ethanol.

Steady-State Fluorescence Spectra. Fluorescence of AAQ was quenched efficiently by the addition of various alcohols and hydroperoxides as observed in the case of ethanol, while absorption spectra were little influenced. In addition, fluorescence spectra showed substantial red shifts (Figure 2). Twenty-six alcohols were examined. The red shift on addition of each alcohol was plotted against the concentration of alcohol in the inset of Figure 2. Very interestingly, the plot afforded a simple line that involves all the data from various alcohols at different concentrations. Hydroperoxides also offered the data on the line. This suggests that all the alcohols behave in a similar manner and that hydroperoxides also simply act as alcohols in the fluorescence-quenching processes. We then examined the difference of quenching efficiency for various alcohols and hydroperoxides. The Stern−Volmer analysis is written as

$$\frac{\Phi_{F0}}{\Phi_F} = 1 + k_q\tau[\mathrm{ROH}] = 1 + K_{sv}[\mathrm{ROH}] \qquad (1)$$

Here, Φ_{F0}, Φ_F, k_q, and τ are fluorescence quantum yield in the absence and presence of quencher, quenching rate constant, and fluorescence lifetime in benzene, respectively. The apparent Stern−Volmer constant (K_{sv}) of 2AAQ, calculated for fluorescence intensity at λ_{max}, varied from 57.5 ($k_q = 7.7 \times 10^9$ M^{-1} s^{-1}), the maximum value for methanol, to 10.4 ($k_q = 1.4 \times 10^9$ M^{-1} s^{-1}), the minimum value for triphenylmethanol. Fluorescence-quenching efficiencies in terms of the apparent Stern−Volmer constant K_{sv} are shown in Table 1. Fluorescence

TABLE 1: Apparent Stern−Volmer Constants for the Fluorescence Quenching (K_{sv})[a] of 2AAQ and 2PAQ by Alcohols and Hydroperoxides and Contact Molecular Surface Area[b] of Hydroxyl Hydrogen (MS(O*H*)) of Quenchers

		K_{sv} (M^{-1})				K_{sv} (M^{-1})	
	MS(O*H*) (Å)	2AAQ	2PAQ	MS(O*H*) (Å^2)	2AAQ	2PAQ
−OH	6.44	57.5	52.4	 4.36	32.9	27.5
	5.82	46.7	40.0	 4.15	23.7	27.7
	5.82	45.2	62.3	 2.91	20.5	31.7
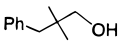	5.40	23.1	31.8	 2.29	10.4	23.0
	5.81	50.8				
	4.78	24.4	29.3	CD_3OD		42.2
	4.99	37.9	31.1	CD_3OH		52.7
	3.95	31.0	39.3	C_2H_5OD		35.0
	4.57	32.9	35.4			19.4
	8.30	69.4	81.6	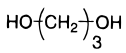 11.2	112	110
	8.30	70.9	81.4	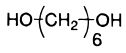 11.2	98.3	94.8
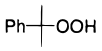	6.23	40.0	48.7	 6.44	54.4	66.0

[a] Apparent Stern−Volmer constants obtained from fluorescence λ_{max} intensity. [b] Gavezzotti/PcMol van der Waals radii (H, 1.15 Å; C, 1.75 Å; N, 1.55 Å; O, 1.40 Å; F, 1.30 Å) and MS-DOT algorithm were used in the ARVOMOL program, and the probe radius is fixed to 1.40 ×81Å.

lifetimes of 2AAQ and 2PAQ were also measured. The lifetimes were shortened on addition of alcohols and hydroperoxides. The Stern−Volmer constants of lifetime measurements coincide well with those of steady-state fluorescence quenching.[20] These results clearly indicate that the fluorescence quenching by alcohols and hydroperoxides is almost a dynamic process. Deuterium isotope effects of the hydroxyl hydrogen of alcohols were appreciably observed in the K_{sv}'s among methanol (K_{sv}(OH)/K_{sv}(OD) = 1.24), ethanol (K_{sv}(OH)/K_{sv}(OD) = 1.14), and triphenylmethanol (K_{sv}(OH)/K_{sv}(OD) = 1.19), while deuteration of the methyl group of methanol did not affect K_{sv} at all (Table 1). The hydroxyl group is indicated to play a crucial role in the fluorescence quenching.

Steric and Electronic Factors in Fluorescence Quenching. Obviously, primary alcohols have larger Stern−Volmer constants, while secondary and tertiary alcohols were less effective for the fluorescence quenching. The difference in quenching efficiency would reflect the molecular properties of quenchers and be mainly ascribable to (1) the electronic factor and (2) the steric one. One of the typical experimental indexes of the electronic factor of the hydroxyl group might be the pK_a value. Any definite correlation, however, between the K_{sv}'s and pK_a's of the examined alcohols and hydroperoxides was not observed at all.[21] The hydrogen bond donor acidity (α) introduced by Kamlet and Taft showed good correlation with the fluorescence-quenching efficiency, though the data points were limited to four kinds of liquid monoalcohols.[22] Those results suggest that the steric factor predominates over the electronic one in the fluorescence quenching, since the p*K*a's are defined as acid−base equilibrium against the water molecule, while the intermolecular hydrogen bonding requires an orientation of the hydroxyl hydrogen toward the carbonyl oxygen atom of AAQ's, which are inherently bulky molecules for the alcohols and hydroperoxides. We need some other appropriate indexes that involve the steric factor also. The chemical shift of ^{13}C NMR might be one of the candidates. The chemical shift of ^{13}C NMR reflects mainly electron density[23] and simultaneously does type and number of substituents also. As shown in Figure 3, a good correlation between the fluorescence quenching efficiency and the ^{13}C NMR chemical shift of carbinol carbon was observed. For the more microscopic molecular index for the steric factor, here we use a concept of contact molecular surface area, which had been originally used in biochemistry, especially for interpretation of protein structures.[24] Some attempts on quantitative treatment of molecular properties such as solubility, viscosity, and the heat of vaporization were reported by calculating molecular volumes and molecular surfaces.[25] The contact surface area of only hydroxyl hydrogen (MS(O*H*)), which should be responsible for the intermolecular hydrogen bond and is accessible by the carbonyl oxygen of AAQ was calculated (see Experimental Section). The MS(O*H*) is largely dependent on the rest of the atoms within the molecule as shown in Table 1. Primary alcohols have the largest contact molecular

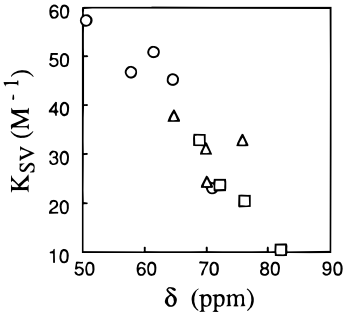

Figure 3. Correlation between apparent Stern−Volmer constants of the fluorescence quenching (K_{sv}) of 2AAQ and ^{13}C chemical shift of carbinol carbon in $CDCl_3$: (○) primary alcohols; (△) secondary alcohols; (□) tertiary alcohols.

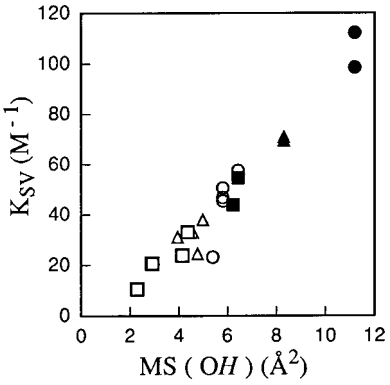

Figure 4. Correlation between apparent Stern−Volmer constants of the fluorescence quenching (K_{sv}) of 2AAQ and contact molecular surface area of hydroxyl hydrogen (MS(O*H*)) of quenchers: (○) primary alcohols; (△) secondary alcohols; (□) tertiary alcohols; (●) 1,3-propanediol and 1,6-hexanediol; (▲) *cis*- and *trans*-1,2-cyclohexanediol; (■) hydroperoxides.

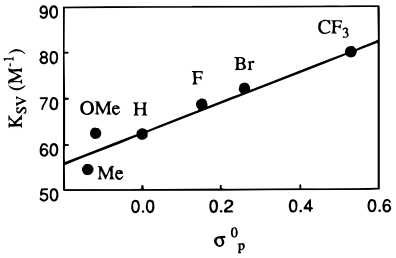

Figure 5. Hammet plot for apparent Stern−Volmer constants of the fluorescence quenching (K_{sv}) of 2PAQ by para-substituted benzyl alcohols.

surface area, while tertiary alcohols have the smallest ones. Hydroperoxides have rather large contact surface areas as anticipated from their structures where the hydroxyl hydrogen is more exposed outside than alcohols owing to the presence of another adjacent oxygen atom. The correlation between the fluorescence-quenching efficiency and contact molecular surface areas is shown in Figure 4. Very good correlation was obtained. The results show that the larger the contact surface area of the exposed hydroxyl hydrogen itself, the greater the quenching efficiency. Hydroperoxides also afforded the data on the line (Figure 4), indicating again that they simply act as alcohol molecules. In the case of hydrogen-bonding interaction, the formation of a hydrogen bond is difficult when hydroxyl hydrogen is sterically hindered. Thus, contact molecular surface area can be a good parameter of steric hindrance.

Though pK_a values of alcohols and hydroperoxides had apparently no correlation with the fluorescence quenching, correlation was again examined among a series of *para*-substituted benzyl alcohols that have almost the same contact surface area and the same steric factors. The Hammet plot for 2PAQ is shown in Figure 5.[26] Substitution by an electron-withdrawing group enhanced the fluorescence quenching. A good linear relationship was obtained. This indicates that benzyl alcohols act as a hydrogen-bonding donor.

All the results obtained above clearly demonstrates that the fluorescence quenching by alcohols and hydroperoxides is directly correlated with the specific intermolecular interaction between the hydroxyl hydrogen of alcohols and the carbonyl oxygen of AAQ. The interaction can be concluded as an intermolecular hydrogen bonding between the carbonyl oxygen and hydroxyl group of alcohols or hydroperoxides. Steric effects on excited-state chemistry have been studied for many photochemical processes such as energy transfer,[27] electron transfer,[28] exciplex formation,[29] and other reactions.[30] Generally, the

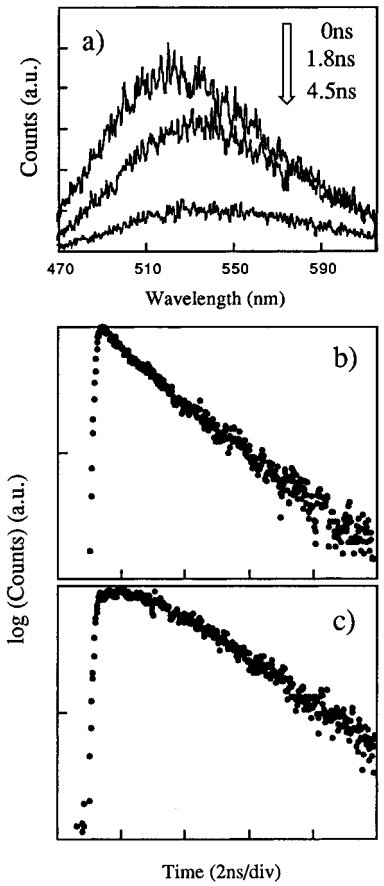

Figure 6. (a) Time-resolved fluorescence spectra of 2AAQ with 0.05 M ethanol at 0s, 1.8, and 4.5 ns after excitation. Gate width is 0.4 ns. (b) Fluorescence decay profiles in short (475−495 nm) wavelength region. (c) Fluorescence decay profiles in long (601−621 nm) wavelength region.

extent of steric effects is more evident in the gas-phase rather than in solution where many collisions within the solvent cage would mask the effect.[31] In excited energy-transfer processes, the steric effects are more profound in the triplet excited state than in the singlet one.[32] The triplet state energy transfer that proceeds through a Dexter type electron exchange mechanism requires overlapping of orbitals between the two chromophores. As easily understood, intermolecular interaction, which requires proximity between the two molecules such as in intermolecular hydrogen bonding, makes the steric effects more evident. The chemical shift of ^{13}C NMR and contact molecular surface area of hydroxyl hydrogen can be good quantitative parameters for the steric effect as demonstrated in the present case.

Time-Resolved Fluorescence Spectra. Fluorescence-quenching dynamics were studied by time-resolved spectroscopy. As described earlier, the Stern−Volmer constant for steady-state fluorescence and fluorescence lifetime (all emission) agreed well within experimental error. In detail, however, more complex decay phenomena were observed. As shown in Figure 2, the steady-state fluorescence spectra on addition of ethanol normalized at their λ_{max} intensities indicated that new emission appeared in the long wavelength region to induce the shift of the fluorescence λ_{max} to the red. Similar tendencies were also observed in other alcohols and hydroperoxides. In accord with the steady-state fluorescence spectra, time-resolved fluorescence spectra of 2AAQ on addition of ethanol also exhibited a red shift of their λ_{max} during the decay (Figure 6). Obviously, new emission has appeared in the long wavelength region. Fluorescence decay in the shorter wavelength region (475−495 nm) showed two-component decay profiles, and clear rise and decay

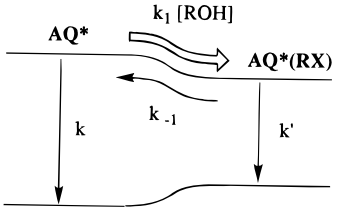

Figure 7. Two emissive excited states diagram including original fluorescent state AQ* and relaxed emissive state AQ*(RX). The rate constants k, k_1, k_{-1}, and k' denote the deactivation rate constant from AQ* to the ground state, the forward relaxation rate constant from AQ* to AQ*(RX), the backward process from AQ*(RX) to AQ*, and the deactivation rate constant from AQ*(RX) to the ground state, respectively.

profiles were observed at longer wavelengths (601−621 nm) one (Figure 6). Steady-state fluorescence in rigid ethanol at 77 K afforded substantial information about the new emission. The λ_{max} of fluorescence of 2PAQ in rigid ethanol at 77 K (580 nm) was much shorter than in fluid ethanol at room temperature (674 nm) and was almost the same as that in benzene at room temperature (584 nm). Similar tendencies were also observed in the case of 2AAQ, though the λ_{max} in rigid ethanol (550 nm) was a little longer than in benzene (527 nm) but much shorter than in fluid ethanol at room temperature (631 nm).

These results strongly suggest that the new emission that appeared in the long wavelength region is ascribable to reorganization of the surrounding solvent ethanol. In the presence of ethanol in benzene solution, reorganization of ethanol to the excited AAQ to form a relaxed intermolecular hydrogen-bonded excited state would induce the new emission in the long wavelength region.

Rate Constants of Fluorescence Quenching. All the results obtained above clearly show that this system is described well by assuming two emitting levels such as the original fluorescent state in benzene AQ*, which is close to the Franck−Condon state, and the less emissive relaxed state AQ*(RX) as shown in Figure 7. The alcohols or hydroperoxides would be strongly hydrogen bonded to the carbonyl of AAQ in the relaxed state AQ*(RX). Time dependencies of these state populations are expressed as in eqs 2−7:[33]

$$[\mathrm{AQ^*}](t) = A\exp(-\lambda_1 t) + B\exp(-\lambda_2 t) \tag{2}$$

$$[\mathrm{AQ^*(RX)}](t) = C\{\exp(-\lambda_1 t) - \exp(-\lambda_2 t)\} \tag{3}$$

$$A = \left(\frac{k + k_1[\mathrm{ROH}] - \lambda_2}{\lambda_1 - \lambda_2}\right)[\mathrm{AQ^*}]_0 \tag{4}$$

$$B = \left(\frac{\lambda_1 - k - k_1[\mathrm{ROH}]}{\lambda_1 - \lambda_2}\right)[\mathrm{AQ^*}]_0 \tag{5}$$

$$C = \frac{(k + k_1[\mathrm{ROH}] - \lambda_1)(\mathrm{k} + \mathrm{k}_1[\mathrm{ROH}] - \lambda_2)}{\mathrm{k}_{-1}(\lambda_1 - \lambda_2)}[\mathrm{AQ^*}]_0 \tag{6}$$

$$\lambda_{1,2} = 0.5\{k + k_1[\mathrm{ROH}] + k_{-1} + k' \mp \sqrt{(k + k_1[\mathrm{ROH}] - k_{-1} - k')^2 + 4k_{-1}k_1[\mathrm{ROH}]}\} \tag{7}$$

where $[\mathrm{AQ^*}]_0$ denotes the initial concentration of AQ* just after the laser pulse and k, k_1, k, and k' are rate constants in Figure 7. Then eqs 2−7 give the following relationship for the time constants λ_1 and λ_2 (eqs 8 and 9):

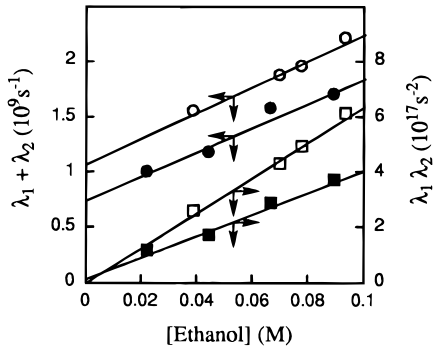

Figure 8. Concentration dependence of the time constant for 2PAQ with ethanol or ethanol-*O*-*d*: (○) $\lambda_1 + \lambda_2$ (ethanol); (●) $\lambda_1 + \lambda_2$ (ethanol-*O*-*d*); (□) $\lambda_1\lambda_2$ (ethanol); (■) $\lambda_1\lambda_2$ (ethanol-*O*-*d*)).

$$\lambda_1 + \lambda_2 = k + k_{-1} + k' + k_1[\mathrm{ROH}] \tag{8}$$

$$\lambda_1\lambda_2 = k(k_{-1} + k') + k'k_1[\mathrm{ROH}] \tag{9}$$

The individual rate constant can be estimated by observing the concentration dependence of time constants λ_1 and λ_2. We tried to estimate these rate constants for the 2AAQ−ethanol system and the 2PAQ−ethanol or −ethanol-*O*-*d* system. It would be expected that in the short wavelength region, emission is mainly from the original fluorescent state in benzene and in the long wavelength region emission is mainly from the RX state, though both the emissions are superimposed with each other over the entire wavelength region. Owing to a limited signal-to-noise ratio in the short wavelength region where the fluorescence from the RX state is by far the weaker than in the long wavelength region, concentration dependencies of the time constants were examined for the data of long wavelength region. The results are shown in Figure 8 and Table 2. The plot of Figure 8 suggests that the data k_1, k' obtained from the slope are more reliable than the data $(k_{-1} + k')$ from the intercept, which has an appreciable error inherently.[34] Thus, the rate constant k_{-1} was estimated by the following procedure. Supposing the fluorescence-quenching scheme is as in Figure 7, the Stern−Volmer equation (eq 1) of steady-state fluorescence quenching should be modified to give eq 10.[35]

$$\frac{\Phi_{\mathrm{F0}}}{\Phi_{\mathrm{F}}} = \frac{1 + \dfrac{k_1k'}{k(k_{-1} + k')}[\mathrm{ROH}]}{1 + \dfrac{k_{\mathrm{F}}'k_1}{k_{\mathrm{F}}(k_{-1} + k')}[\mathrm{ROH}]} \tag{10}$$

where $k = k_{\mathrm{F}} + k_{\mathrm{NR}}$, $k' = k_{\mathrm{F}}' + k_{\mathrm{NR}}(\mathrm{RX})$ with k_{F} and k_{F}' being the radiative rate constants of the original fluorescent state and the relaxed state, respectively. k_{NR} and $k_{\mathrm{NR}}(\mathrm{RX})$ denote nonradiative rate constants of the original fluorescent state and the relaxed state, respectively. The good linear Stern−Volmer plot in each case[36] strongly suggests that the term $[k_{\mathrm{F}}'k_1/(k_{\mathrm{F}}(k_{-1} + k'))][\mathrm{ROH}]$ in the denominator of eq 10 is negligible and that the equation can be written as

$$\frac{\Phi_{\mathrm{F0}}}{\Phi_{\mathrm{F}}} = 1 + \frac{k_1k'}{k(k_{-1} + k')}[\mathrm{ROH}] \tag{11}$$

Thus, the Stern−Volmer constant K_{sv} in eq 1 leads to the relation $K_{\mathrm{sv}} = k_{\mathrm{q}}/k = k_1k'/(k(k_{-1} + \mathrm{k}'))$. The apparent quenching rate constant k_{q} obtained in steady-state fluorescence quenching is

TABLE 2: Rate Constants in Fluorescence Quenching of AAQ by Ethanol[a]

	quencher	k_1 (10^{10} M^{-1} s^{-1})[b,c]	k' (10^8 s^{-1})[b,d]	k_q (10^9 M^{-1} s^{-1})[e]	k_{-1} (10^8 s^{-1})[f]
2AAQ	ethanol	0.98	6.4	6.2	3.7
2PAQ	ethanol	1.2	5.3	4.2	9.6
	ethanol-*O*-*d*	1.1	3.5	3.7	7.1

[a] k values in benzene are 1.3×10^8 s^{-1} (2AAQ) and 1.1×10^8 s^{-1} (2PAQ), respectively. [b] Fluorescence decays of 2AAQ (601−621 nm) and 2PAQ (660−680 nm) were analyzed. [c] Obtained from the slope of $\lambda_1 + \lambda_2$ vs [ROH] plot. [d] Obtained from the slope of $\lambda_1\lambda_2$ vs [ROH] plot. [e] Apparent fluorescence quenching rate constant obtained from eq 1 for λ_{max} intensity. [f] Calculated by eq 12.

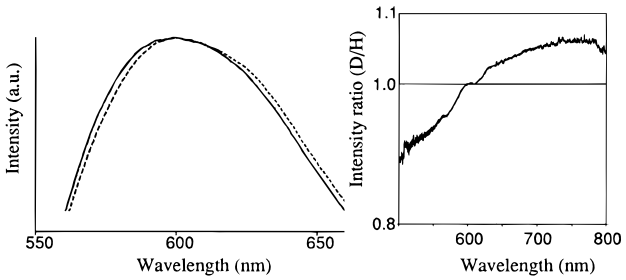

Figure 9. (Left) Fluorescence spectra of 2PAQ with ethanol in benzene, where the intensity was normalized at λ_{max}: (solid line) 0.05 M ethanol; (broken line) 0.05 M ethanol-*O*-*d*). (Right) Ratio (ethanol-*O*-*d*/ethanol) of normalized spectra.

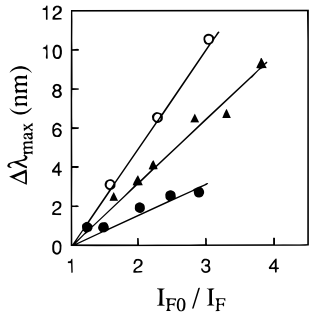

Figure 10. Fluorescence λ_{max} of 2AAQ on addition of ethanol (○), 1,3-propanediol (●), and 1,2-cyclohexanediol (▲) against quenching ratio (I_{F0}/I_F).

thus expressed as eq 12

$$k_q = \frac{k_1 k'}{k_{-1} + k'} \tag{12}$$

The backward process k_{-1} was thus calculated from eq 12 by the values of k_q, k_1, and k'. The forward relaxation processes (k_1) forming the hydrogen-bonded states were nearly diffusion controlled,[37] while the backward ones (k_{-1}) were almost negligible compared with k_1. The decay rate constant from the RX state of 2AAQ (k') was about 5 times larger than the decay rate constant k in benzene.

The deuterium isotope effect was examined in the case of 2PAQ, which has no NH bond and suffers no deuteration of the amino substituent in contrast to 2AAQ.[2] Ethanol-*O*-*d* was used for the quencher, and the obtained rate constants are compared in Table 2. A moderate deuterium isotope effect was observed on k' ($k'_{OH}/k'_{OD} = 1.5$). The effect may reflect the difference in Franck−Condon factor between ═O···H─O─ and ═O···D─O─ in the radiationless transition through the intermolecular hydrogen bond. Interestingly, the deuterium isotope effect was also observed in the shape of the fluorescence spectrum on addition of ethanol-*O*-*d* or ethanol-*O*-*h*. The normalized spectra are compared in Figure 9. The relative intensity in the long wavelength region on addition of ethanol-*O*-*d* was stronger than in the case of ethanol-*O*-*h*. This is well rationalized by the larger contribution of the new emission in the long wavelength region due to the longer lifetime ($1/k'$) of the RX state in the case of ethanol-*O*-*d*.

Here, we could recognize a very crucial point. The deactivations from the RX state in benzene (k') were 6.4×10^8 s^{-1} for 2AAQ and 5.3×10^8 s^{-1} for 2PAQ, by far slower than those in neat ethanol, 1.9×10^{10} s^{-1} ($\tau = 54$ ps for 2AAQ) and 2.5×10^{10} s^{-1} ($\tau = 40$ ps for 2PAQ).[2] Though the emitting state in neat ethanol is a relaxed hydrogen-bonded excited state,[38] the discrepancy between the deactivation in benzene and ethanol might be too large for a simple difference of solvent character such as polarity. It strongly suggests that the hydrogen-bonded excited states of AAQ are not necessarily the same but have a different nature in benzene and ethanol. In benzene solution unimolecular collision of ethanol would induce the formation of the relaxed hydrogen-bonded excited state, while in neat ethanol AAQ are all surrounded by plural ethanol molecules, and more than one ethanol molecule may play important roles in the deactivation.

Fluorescence Quenching by Diol. To get more information about the above point, fluorescence quenchings by diols, which have two hydroxyl groups within one molecule, were further examined. 1,3-Propanediol as a flexible diol and *cis*- and *trans*-1,2-cyclohexanediol as rigid diols were used, and the results were compared with other monoalcohols. As expected, the contact molecular surface areas (MS(O*H*)) of the diols were calculated to be almost as doubled as with those of monoalcohols (Table 1). Stern−Volmer constants of steady-state fluorescence quenching in benzene were also well correlated with the MS(O*H*) as indicated in Figure 4. Any characteristic difference was not observed in the Stern−Volmer constant among monoalcohols and diols. A striking difference, however, evidently appeared in the shape of the fluorescence spectra. Fluorescence λ_{max} of 2AAQ in benzene against relative fluorescence intensities on addition of ethanol, *cis*- and *trans*-1,2-cyclohexanediol, and 1,3-propanediol are compared in Figure 10. As described earlier, the λ_{max} shifted substantially to the red on addition of ethanol owing to the appearance of a new emission band in the long wavelength region, while 1,3-propanediol hardly induced the new emission, and thus, the shift of λ_{max} was very small (Figure 10). Interestingly, the characteristic difference was observed only in the case of 1,3-propanediol, and other diols such as *cis*- and *trans*-1,2-cyclohexanediol exhibited larger spectral shifts as in the case of ethanol. The results suggest that 1,3-propanediol can quench the new emission in the long wavelength region, which has appeared in the cases of other alcohols. The phenomena must be closely related to the deactivation in neat ethanol where efficient quenching is operating owing to a possible participation of more than one ethanol molecule. The results could be plausibly explained as follows. Once the one hydroxyl group of 1,3-propanediol is attached to the carbonyl oxygen of excited AAQ, the second hydroxyl group within the diol molecule presumably attacks the carbonyl oxygen to induce an efficient deactivation. The efficient deactivation leads to a quenching of the new emission in the long wavelength region. Supposing that two hydroxyl groups on the carbonyl oxygen induce an

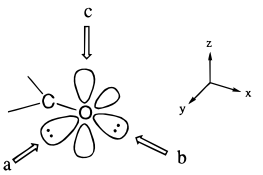

Figure 11. Molecular orbitals of carbonyl group and approaching direction to form the hydrogen bond. a and b are in-plane mode approaches to p_y and sp_x orbitals. c is the out-of-plane mode approach to the p_z orbital.

efficient deactivation, a size fitting between the carbonyl and diol molecule would operate in the process. The geometrical situation of the two hydroxyl groups of 1,3-propanediol may be suitable for seizing the carbonyl oxygen, while *cis*- and *trans*-1,2-cyclohexanediol may have too short distances, and congested hydroxyl group with rigid structure may prevent the second attack of another hydroxyl group on the carbonyl oxygen.

New Emission in the Long Wavelength Region. Simple questions may arise from the results and the speculation above. What is the actual species that causes the new emission in the long wavelength region? What is the difference in interactions between the first and the second attack of the hydroxyl group toward the carbonyl oxygen in the case of 1,3-propanediol? As described earlier, 2AAQ and 2PAQ formed hydrogen-bonded complexes upon addition of excess ethanol, though the formation constants were rather small. The new absorption band due to the hydrogen-bonded species appeared in the original absorption edge as indicated by the difference spectra in the inset of Figure 1. Selective excitation of the hydrogen-bonded species in the ground state on addition of excess ethanol induced an emission other than the original fluorescence. The new emission can be safely assigned as the fluorescence from the excited state of the ground-state hydrogen-bonded species of AAQ. Quantum yields of the fluorescence were 0.0023(2AAQ) and 0.0047(2PAQ),[39] 2 orders of magnitude less emissive than the original fluorescence ($\Phi_F = 0.14$ (2AAQ) and 0.13(2PAQ), respectively). The shape and λ_{max} (612 nm, 2AAQ; 644 nm, 2PAQ)[39] of the fluorescence look very similar to those of the new emission in the long wavelength region observed in the steady state and time-resolved fluorescence spectra under the normal conditions ([ethanol] = 0−0.05 M) where the formation of the ground-state hydrogen-bonded complex is negligible. Thus, the relaxed excited state (RX) depicted in Figure 7 could be assigned as the corresponding excited state of the ground-state hydrogen-bonded complex. Since a hydrogen bonding to a ground-state carbonyl oxygen is generally induced on a nonbonding p_y orbital as shown in Figure 11a,[40] the conformation should be the same in the RX state, which is the excited state of the ground-state complex. The relaxation to hydrogen-bonded excited state (RX) thus could be induced by an "in-plane mode attack" of the hydroxyl hydrogen to the carbonyl oxygen of excited AAQ (Figure 11a).

Molecular Mechanism of Fluorescence Quenching. The second question arises here again. What is the difference in interactions between the first and the second attack of the hydroxyl group on the carbonyl oxygen in the case of 1,3-propanediol? The electronic structure of the excited AAQ should be a crucial point. Since the lowest excited state of AAQ has a strong intramolecular charge transfer nature that involves a transition mainly from the π orbital of the amino nitrogen to the π^* orbital localized mainly on the carbonyl group, the total electron density in the excited state is mostly emphasized on the carbonyl oxygen.[41] The second mode attack of the hydroxyl hydrogen would be most plausibly understood as an interaction through the π^* orbital, which may be called an "out-of-plane mode attack" as depicted in Figure 11c. The out-of-plane mode attack was also reported in hydrogen bonding to the fluorenone radical anion.[42] The dual mode interactions in the case of 1,3-propanediol suggests that the phenomena should be closely related to the efficient deactivation in neat ethanol where plural alcohol molecules can participate in the solvent cage. In ethanol, the dual mode interactions of in-plane and out-of-plane are thought to operate simultaneously to lead to very efficient deactivation (Figure 12). These experimental results and discussions further lead to the following speculation. In benzene solution, unimolecular attack of ethanol may not necessarily be predominant in the in-plane mode, but the out-of-plane one is thought to operate also. The unimolecular attack in the out-of-plane mode would form another nonemissive relaxed excited state that suffers very efficient deactivation. All the obtained results and discussions thus could depict Figure 12 as the molecular mechanism of fluorescence quenching.

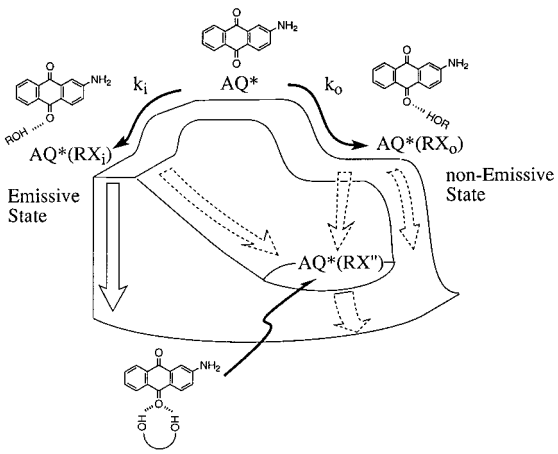

Figure 12. Oversimplified picture of the molecular mechanism of fluorescence quenching. The left path (k_i) represents a relaxation to the emissive state AQ*(RX_i). The right path (k_o) represents a relaxation to the nonemissive state AQ*(RX_o) where the effective deactivation to the ground state is dominant. Relaxation to the AQ*(RX″) could be induced in the case of 1,3-propanediol.

To the original fluorescent state in benzene AQ*, the in-plane mode attack of alcohol (k_i) leads to the formation of the less emissive, relaxed hydrogen-bonded state AQ*(RX_i), which is the excited state of the hydrogen-bonded complex in the ground state. The out-of-plane mode attack (k_o) will form another nonemissive hydrogen-bonded excited state AQ*(RX_o) where the interaction is through the π^* orbital of AAQ. The observed k_1 is thus expressed as $k_1 = k_i + k_o$. The rate constant k' thus represents the deactivation from the less emissive, relaxed excited state (RX_i), which is hydrogen-bonded by the in-plane mode. Since the RX_i state has a moderate lifetime as indicated in Table 2, the first in-plane mode attack by one hydroxyl group in the case of 1,3-propanediol would be followed by the second out-of-plane attack by the other hydroxyl group to form a doubly hydrogen-bonded nonemissive state AQ*(RX″) that suffers an efficient deactivation. On the other hand, supposing the first attack of one hydroxyl group being in the out-of-plane mode, the resultant nonemissive state (RX_o) may not have enough lifetime to suffer the second in-plane-mode attack by the other hydroxyl group of 1,3-propanediol. Since hydroperoxides were demonstrated to behave as alcohols, the out-of-plane mode hydrogen-bonded form, which suffers more efficient deactivation than the in-plane-mode form, would play a crucial role in the sensitized decomposition. The microscopic molecular mechanism of how the hydrogen-bonding interaction causes the fluorescence quenching should be a very crucial point to be clarified. How the excited energy is dissipated through both

modes of in-plane and out-of-plane interactions is most curious. Stabilization of the excited state by hydrogen bonding may alter the radiative and nonradiative processes as discussed by Harriman and Mataga et al.[43] The observed deuterium isotope effect, however, emphasizes again the possibility that the intermolecular hydrogen bond vibration acts as an accepting mode of radiationless transition as previously postulated.[2] The fluorescence quenching of AAQ might be one of the typical examples that show that the microscopic molecular process of radiationless deactivation is not necessarily isotropic but inherently anisotropic in general. Investigations of a similar process in aminofluorenone derivatives are now in progress. Only one carbonyl group within the molecule in the case of aminofluorenones would be expected to exhibit the phenomena in a more explicit manner.

Conclusion

Fluorescence quenching of AAQ by alcohols and hydroperoxides through intermolecular hydrogen-bonding interaction was found to be one of typical systems for studying the microscopic molecular mechanism of radiationless deactivation. The quenching phenomenon was successfully explained by steric factors mainly ascribable to the hydroxyl group of alcohols. The contact molecular surface area of the hydroxyl hydrogen was revealed to be a good index for the steric factors. Deactivation of excited AAQ proceeded through dual modes of interaction between the carbonyl oxygen of AAQ and the hydroxyl group of alcohols. In-plane-mode attack of hydroxyl hydrogen toward carbonyl oxygen results in the formation of an emissive hydrogen-bonded complex in the excited state, and an out-of-plane-mode attack induces an efficient deactivation to the ground state.

Acknowledgment. This work was partly defrayed by a Grant-in Aid from the Ministry of Education, Science, Sports, and Culture of Japan and also by Tokyo Ohka Foundation for the Promotion of Science and Technology.

References and Notes

(1) Turro, N. J. *Modern Molecular Photochemistry*; University Science Books: Mill Valley, CA, 1991; p 132.

(2) Inoue, H.; Hida, M.; Nakashima, N.; Yoshihara, K. *J. Phys. Chem.* **1982**, *86*, 3184.

(3) Miyasaka, H.; Tabata, A.; Kamada, K.; Mataga, N. *J. Am. Chem. Soc*. **1993**, *115*, 7335.

(4) Miyasaka, H.; Tabata, A.; Ojima, S.; Ikeda, N.; Mataga, N. *J. Phys. Chem*. **1993**, *97*, 8222.

(5) Tanaka, F.; Kato, M.; Mataga, N. *Z. Phys. Chem.* **1970**, *70*, 104.

(6) Sessler, J. L; Wang, B.; Harriman, A. *J. Am. Chem. Soc*. **1995**, *117*, 704.

(7) Borst, H. U.; Kelemen, J.; Fabian, J.; Nepras, M.; Kramer, H. E. A. *J. Photochem. Photobiol. A* **1992**, *69*, 97. Ritter, J.; Borst, H. U.; Lindner, T.; Hauser, M.; Brosig, S.; Bredereck, K.; Steiner, U. E.; Kühn, D.; Kelemen, J.; Kramer., H. E. A. *J. Photochem. Photobiol. A* **1988**, *41*, 227.

(8) Srivatsavoy, V. J. P.; Venkataraman, B.; Periasamy, N. *J. Photochem. Photobiol. A* **1992**, *68*, 169. Srivatsavoy, V. J. P.; Venkataraman, B.; Periasamy, N. *Proc. Indian Acad. Sci., Chem. Sci.* **1992**, *104*, 731.

(9) Flom, S. R.; Barbara, P. F. *J. Phys. Chem.* **1985**, *89*, 4489.

(10) Jones, G., II; Feng, Z.; Bergmark, W. R. *J. Phys. Chem*. **1994**, *98*, 4511.

(11) Lin, S.; Struve, W. S. *J. Phys. Chem.* **1991**, *95*, 2251.

(12) Moog, R. S.; Burozski, N. A.; Desai, M. M.; Good, W. R.; Silvers, C. D.; Thompson, P. A.; Simon, J. D. *J. Phys. Chem.* **1991**, *95*, 8466.

(13) Inoue, H.; Yatsuhashi, T.; Shiragami, T.; Luo, Ji. XVth IUPAC Symposium on Photochemistry, Prague, 1994; Abstract p 64. Yatsuhashi, T.; Inoue, H. XVIth IUPAC Symposium on Photochemistry, Helsinki, 1996; Abstract p 598.

(14) Klessinger, M.; Michl, J. *Excited States and Photochemistry of Organic Molecules*; VCH: New York, 1995; p 320.

(15) Perrin, D. D.; Armarego, W. L. F. *Purification of Laboratory Chemicals*, 3rd ed.; Pergamon Press: New York, 1988.

(16) Richard, F. M. *Annu. Rev. Biophys. Bioeng.* **1977**, *6*, 151.

(17) Gavezzotti, A. *J. Am. Chem. Soc.* **1983**, *105*, 5220.

(18) Fernandez Pacios, L. *ARVOMOL*, Version 2; QCPE Program 132, 1994; Department Quimica y Bioquimica ETIS, Montes University Politecnica de Madrid: Madrid, 1994.

(19) Connolly, M. L. *J. Am. Chem. Soc.* **1985**, *107*, 1118.

(20) In the case of 2AAQ with ethanol as a typical case, the fluorescence decay of almost the whole spectral region (480−610 nm) was fitted as a single-exponential decay and the Stern−Volmer constant for the lifetime was obtained as 38.4. The Stern−Volmer constant for fluorescence quantum yield was calculated to be 36.6.

(21) The pK_a values (in water at 25 °C) of quenchers were 15.1 (methanol), 15.9 (ethanol), 15.4 (benzyl alcohol), and 17.1 (2-propanol) from Hurto, J. *Acta Chem. Scand.* **1964**, *18*, 1043, 15.6 (diphenylmethanol) and 16.8 (*tert*-butyl alcohol) from Takahashi, S.; Cohen, L. A.; Miller, H. K.; Peake, E. G. *J. Org. Chem.* **1971**, *36*, 1205, 15.5 (2-phenyl-2-propanol) and 13.2 (triphenylmethanol) from Yuan, L.; Bruice, T. C. *J. Am. Chem. Soc.* **1985**, *107*, 512 (Figure 1), and 12.6 at 20 °C (cumenhydroperoxide) and 12.8 (*tert*-butylhydroperoxide) from Richardson, W. H.; Hodge, V. F. *J. Org. Chem.* **1970**, *35*, 4012.

(22) K_{sv} were plotted against the α value of methanol (0.93), ethanol (0.83), 2-propanol (0.76), and *tert*-butyl alcohol (0.68). The correlation coefficients were 0.98 (2AAQ) and 0.96 (2PAQ). The α values were taken from the following. Taft, R. W.; Kamlet, M. J. *J. Am. Chem. Soc.* **1976**, *98*, 2886. Kamlet, M. J.; Abboud, J. M.; Abraham, M. H.; Taft, R. W. *J. Org. Chem.* **1983**, *48*, 2877. Reichardt, C. *Solvents and Solvent Effects in Organic Chemistry*; VCH: Weinheim, 1988; Chapter 7.

(23) Kalinowski, H. O.; Berger, S.; Braun, S. *Carbon-13 NMR Spectroscopy*; John Wiley & Sons: Chichester, U.K., 1988; Chapter 3.

(24) Lee, B.; Richards, F. M. *J. Mol. Biol.* **1971**, *55*, 379. Connolly, M. L. *Science* **1983**, *221*, 709.

(25) Valvani, S. C.; Yalkowsky, S. H.; Amidon, G. L. *J. Phys. Chem.* **1976**, *80*, 829. Meyer, A. Y. *J. Comput. Chem.* **1986**, *7*, 144.

(26) Hammet's σ^0_p values obtained from the following. Ehrenson, S.; Brownlee, R. T. C.; Taft, R. W. *Prog. Org. Chem.* **1973**, *10*, 1. Isaacs, N. S. *Physical Organic Chemistry*; Longman Science & Technical: Essex, U.K., 1987; p 134. Electron densities of the hydroxyl hydrogen calculated by MOPAC (94.10 PM3) were well correlated with the apparent Stern−Volmer constants and also with the σ^0_p value. The correlation coefficients were 0.91 and 0.96, respectively.

(27) Herkstroeter, W. G.; Hammond, G. S. *J. Am. Chem. Soc.* **1966**, *88*, 4769. Loper, G. L.; Lee, E. K. C. *J. Chem. Phys.* **1975**, *63*, 264.

(28) Gould, I. R.; Farid, S. *J. Phys. Chem.* **1993**, *97*, 13067, and references therein.

(29) A series of exciplex kinetics were studied by Ware. Cheung, S. T.; Ware, W. R. *J. Phys. Chem.* **1983**, *87*, 466, and reference therein.

(30) Matsuura, T. *Kagaku no Ryoiki* **1969**, *23*, 858; **1969**, *23*, 957.

(31) Yekta, A.; Turro, N. J. *Chem. Phys. Lett.* **1972**, *17*, 31.

(32) Wamser, C. C.; Medary, R. T.; Kochevar, I. E.; Turro, N. J. *J. Am. Chem. Soc.* **1975**, *97*, 4864.

(33) Birks, J. B. *Photophysics of Aromatic Molecules*; Wiley: London, 1970; Chapter 7.

(34) The rate constants k_{-1}, obtained from the $\lambda_1 + \lambda_2$ and $\lambda_1\lambda_2$ plots, did not agree well with each other owing to the low fluorescent quantum yield of the RX state. The intercept of the $\lambda_1\lambda_2$ plot has a large error, since the value is nearly zero as shown in Figure 8.

(35) Mataga, N.; Kubota, T. *Molecular Interactions and Electronic Spectra*; Marcel Dekker: New York, 1970; Chapter 7.

(36) The correlation coefficient was greater than 0.995 in each case.

(37) The diffusion-controlled rate constant is 1.1×10^{10} M s^{-1} in benzene at 25 °C. Murov, S. L.; Carmichael, I.; Hug, G. L. *Handbook of Photochemistry*, 2nd ed.; Marcel Dekker: New York, 1993; Section 7.

(38) Supposing the forward rate constant (k_1) to be also diffusion controlled in neat ethanol and the concentration of ethanol to be estimated as [ethanol] = 17 M, a simple calculation of the process (k_1[ethanol]) would give $1 \times 10^{10} \times 17 = 1.7 \times 10^{11}$ s^{-1}, which is almost 10 times larger than the observed deactivation rate constants in ethanol. It strongly suggests that the rate-determining step of fluorescence decay in ethanol is the deactivation from the relaxed hydrogen-bonded excited state.

(39) In the presence of 1.0 M ethanol, the newly appeared absorption band was selectively excited at 500 nm (2AAQ) and 560 nm (2PAQ).

(40) Nonbonding electrons of carbonyl were located on the p_y (Figure 11a) and sp_x orbitals (Figure 11b), but the energy level of the latter is lower than the former. Orchin, M.; Jaffe, H. H. *The importance of antibonding orbitals*; Houon Mifin Company: Boston, 1967.

(41) Inoue, H.; Hoshi, T.; Yoshino, J.; Tanizaki, Y. *Bull. Chem. Soc. Jpn*. **1972**, *45*, 1018; **1973**, *46*, 380.

(42) Ichikawa, T.; Ueda, K.; Yoshida, H. *Bull. Chem. Soc. Jpn.* **1991**, *64*, 2695.

(43) Brun, A. M.; Harriman, A.; Tsuboi, Y.; Okada, T.; Mataga, N. *J. Chem. Soc. Faraday Trans.* **1995**, *91*, 4047.